

## Kinesin spindle protein (KSP) inhibitors. Part 2: The design, synthesis, and characterization of 2,4-diaryl-2,5-dihydropyrrole inhibitors of the mitotic kinesin KSP

Mark E. Fraley,<sup>a,\*</sup> Robert M. Garbaccio,<sup>a</sup> Kenneth L. Arrington,<sup>a</sup> William F. Hoffman,<sup>a</sup> Edward S. Tasber,<sup>a</sup> Paul J. Coleman,<sup>a</sup> Carolyn A. Buser,<sup>b</sup> Eileen S. Walsh,<sup>b</sup> Kelly Hamilton,<sup>b</sup> Christine Fernandes,<sup>b</sup> Michael D. Schaber,<sup>b</sup> Robert B. Lobell,<sup>b</sup> Weikang Tao,<sup>b</sup> Victoria J. South,<sup>b</sup> Youwei Yan,<sup>c</sup> Lawrence C. Kuo,<sup>c</sup> Thomayant Prueksaritanont,<sup>d</sup> Cathy Shu,<sup>d</sup> Maricel Torrent,<sup>a</sup> David C. Heimbrook,<sup>b</sup> Nancy E. Kohl,<sup>b</sup> Hans E. Huber<sup>b</sup> and George D. Hartman<sup>a</sup>

<sup>a</sup>Department of Medicinal Chemistry, Merck Research Laboratories, West Point, PA 19486, USA

<sup>b</sup>Department of Cancer Research, Merck Research Laboratories, West Point, PA 19486, USA

<sup>c</sup>Department of Structural Biology Merck Research Laboratories, West Point, PA 19486, USA

<sup>d</sup>Department of Drug Metabolism, Merck Research Laboratories, West Point, PA 19486, USA

Received 4 November 2005; revised 5 January 2006; accepted 6 January 2006

Available online 24 January 2006

**Abstract**—The evolution of 2,4-diaryl-2,5-dihydropyrroles as inhibitors of KSP is described. Introduction of basic amide and urea moieties to the dihydropyrrole nucleus enhanced potency and aqueous solubility, simultaneously, and provided compounds that caused mitotic arrest of A2780 human ovarian carcinoma cells with EC<sub>50</sub>s < 10 nM. Ancillary hERG activity was evaluated for this series of inhibitors.

© 2006 Elsevier Ltd. All rights reserved.

Mitotic kinesins are microtubule-associated motor proteins that utilize the energy from ATP hydrolysis for bipolar spindle assembly, maintenance and elongation, chromosome alignment and segregation, and microtubule depolymerization, among other functions during cell division.<sup>1</sup> KSP (kinesin spindle protein, *HsEg5*) is a mitotic kinesin that causes centrosome separation, a process required for bipolar spindle formation and maintenance.<sup>2</sup> Inhibition of KSP with small molecules results in collapse of bipolar spindles and gives rise to monopolar spindle arrays, referred to as monoasters.<sup>3</sup> Importantly, this phenotype is accompanied by cell cycle arrest in mitosis, and prolonged mitotic arrest in tumor cells leads to apoptosis.<sup>4,5</sup> KSP inhibitors therefore have potential as general antiproliferative agents useful for the treatment of cancer. Additionally, KSP inhibition

represents a novel and specific mechanism to target the mitotic spindle that may be devoid of the neuropathy-associated, mechanism-based side effects common to the taxanes and other natural products that target microtubules. KSP inhibitors may also offer advantages over these agents with regard to formulation and tumor resistance. Efforts to establish proof-of-concept with ispinesib (SB-715992), a KSP inhibitor of the quinazolinone class,<sup>6</sup> in Phase II clinical trials are currently ongoing. In this communication, we describe the design, synthesis, and evaluation of 2,4-diaryl-2,5-dihydropyrroles as inhibitors of KSP.

We recently reported the development of 3,5-diaryl-4,5-dihydropyrazoles as potent and cell-active KSP inhibitors.<sup>7</sup> These compounds demonstrated high selectivity for KSP versus other kinesins, a consequence of their allosteric mode of binding. Part of our efforts to expand the scope of this series centered on modifications to the core structure designed to improve reactivity in amide bond-forming reactions and to preserve the orientation of the two aryl groups to maintain potency. We rationalized

**Keywords:** KSP; hERG; Dihydropyrroles; Kinesin spindle protein; Antimitotics; Antiproliferative; Anticancer.

\*Corresponding author. Tel.: +1 215 652 6937; fax: +1 215 652 7310; e-mail: [mark\\_fraley@merck.com](mailto:mark_fraley@merck.com)

that a 2,5-dihydropyrrole nucleus might serve as a viable replacement for the 4,5-dihydropyrazole core in that the hybridization of the aryl-bearing carbon atoms would be maintained, allowing for a similar presentation of the diaryl array (Fig. 1). To test this hypothesis, a synthetic route to racemic **1** was developed based on sequential Heck coupling reactions of aryl diazonium intermediates reported by Carpes and Correia (Fig. 2).<sup>8</sup> The substitution pattern selected for the diaryl rings of **1** was found to be optimal for the dihydropyrazole series, and thus was maintained for our exploratory studies in this new series.

Acylation of (+/–)-**1** with acetyl, pivaloyl or dimethylcarbamyl chloride provided dihydropyrrole amides **2** and **4** and urea **6** (following resolution by chiral chromatography), respectively.<sup>9</sup> The KSP inhibitory activity<sup>10</sup> of this initial set of compounds was compared to the corresponding series of dihydropyrazoles, **3**, **5**, and **7** (Table 1). While compound **2** showed lower potency relative to **3**, compounds **4** and **6** compared favorably to their counterparts **5** and **7**, suggesting that branched acyl groups were necessary for potency in the dihydropyrrole series. In addition, the *S* configuration of **6** was determined to be a critical feature of potency,<sup>11</sup> an observation consistent with the stereochemical requirement for potency in the dihydropyrazole series. Having established the dihydropyrrole ring system as a suitable alternative to the dihydropyrazole core, we next devised an

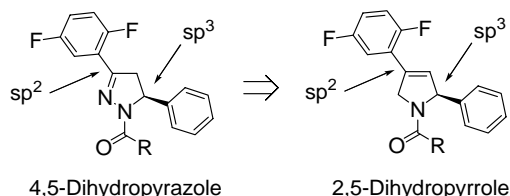


**Figure 1.** Design strategy: maintain hybridization of aryl-substituted carbon atoms.

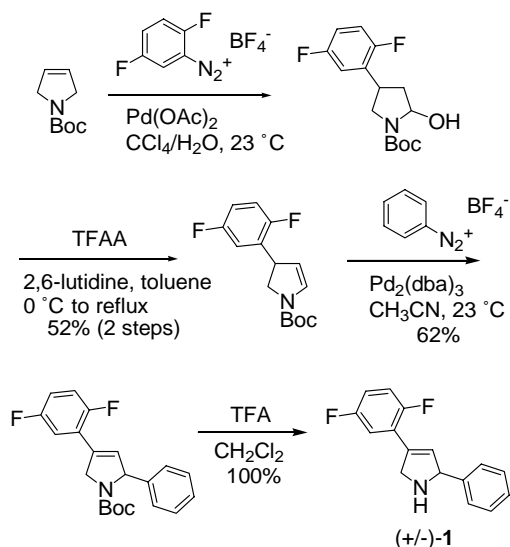


**Figure 2.** Synthesis of (+/–)-**1**.

**Table 1.** KSP inhibitory activity of compounds **2**–**7**

Compound	Core	R	KSP IC <sub>50</sub> (nM)
<b>2</b> (+/–)	A	Me	4000
<b>3</b> (+/–)	B	Me	94
<b>4</b> (+/–)	A	<i>t</i> -Bu	85
<b>5</b> (+/–)	B	<i>t</i> -Bu	113
<b>6</b> (–, <i>S</i> )	A	NMe <sub>2</sub>	38
<b>7</b> (+/–)	B	NMe <sub>2</sub>	84

asymmetric sequence to (*S*)-**1** to support our optimization efforts.

As illustrated in Figure 3, the route began with a one-pot preparation of alcohol **9** from nitrile **8**<sup>12</sup> by the method of Maeda et al.<sup>13</sup> Swern oxidation of **9** followed by regioselective enolization of ketone **10** with NaHMDS<sup>14</sup> and trapping of the resultant enolate with PhNTf<sub>2</sub> furnished enol triflate **11**. Suzuki cross-coupling reaction of **11** with 2,5-difluorophenylboronic acid proceeded smoothly to afford **12**, and removal of the Boc group then provided (*S*)-**1**.

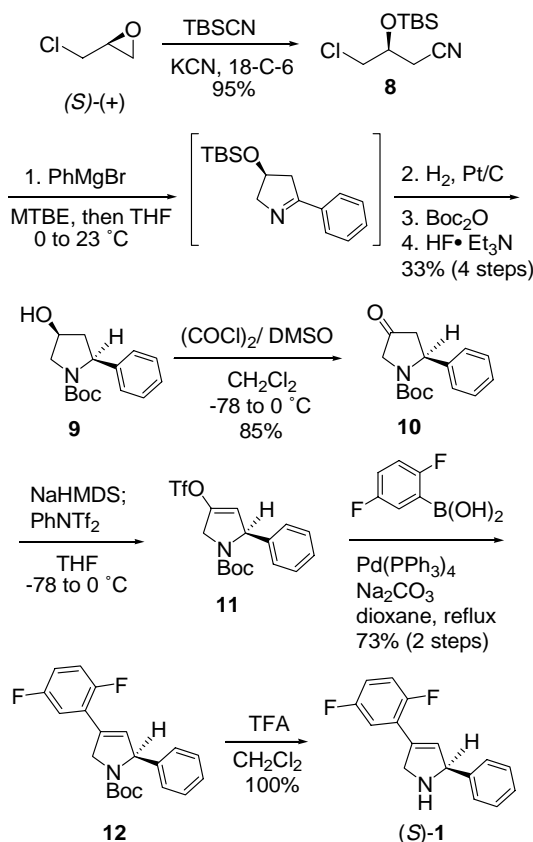


**Figure 3.** Synthesis of (*S*)-**1**.

With (*S*)-**1** in hand, a wide range of branched basic amides and ureas were prepared with the goal of identifying compounds with improved potency and aqueous solubility, important for iv formulation, over leads **4** and **6**. The KSP inhibitory profiles of a select set of compounds, **13–22**, prepared by the methods illustrated in Figure 4, are presented in Table 2.<sup>15</sup> Included are the EC<sub>50</sub> values for mitotic arrest (Cell EC<sub>50</sub>)<sup>16</sup> in A2780 human ovarian carcinoma cells and binding data against the I<sub>Kr</sub> potassium channel hERG (human *Ether-a-go-go* Related Gene).<sup>17</sup> We closely monitored hERG binding in that blockade of this ion channel has been implicated in drug-induced prolongation of the heart-rate corrected QT interval of the ECG, a side effect that can potentiate cardiac arrhythmia and lead to torsades de pointes or even sudden death in extreme cases.<sup>18</sup>

In general, the data for this select set of compounds indicated that incorporation of basic unsymmetrical ureas or branched  $\alpha$ - or  $\beta$ -amino amides provided low molecular weight inhibitors with excellent potency and solubility properties. Specifically, in the urea series, the 4-piperidinyll group of urea **13** proved optimal in terms of potency, cellular activity, and aqueous solubility (>10 mg/mL, pH 5). However, the basicity of **13** conferred binding affinity to hERG, as determined by comparison to the non-basic acylated derivative **14**. In the amide series, a number of highly potent and water soluble inhibitors were identified. Interestingly, in the case of the  $\alpha$ -amino amides, only the *S* configuration of the  $\alpha$ -stereocenter imparted a high level of potency (compare diastereomers **17** and **18**). These basic amides, like the basic ureas, demonstrated moderate levels of hERG binding. The hERG IC<sub>50</sub> value for **19** was corroborated by cellular electrophysiology using a standard whole-cell voltage clamp assay in CHO cells that stably expressed hERG (IC<sub>50</sub> = 6500 nM). As a partial solution to this potential liability, we found that neutral acyl groups, such as those incorporated in **21** and **22**, ameliorated hERG activity without major loss of potency, but at the expense of aqueous solubility. The following paper details strategies to solubilize charge-neutral inhibitors from this series.

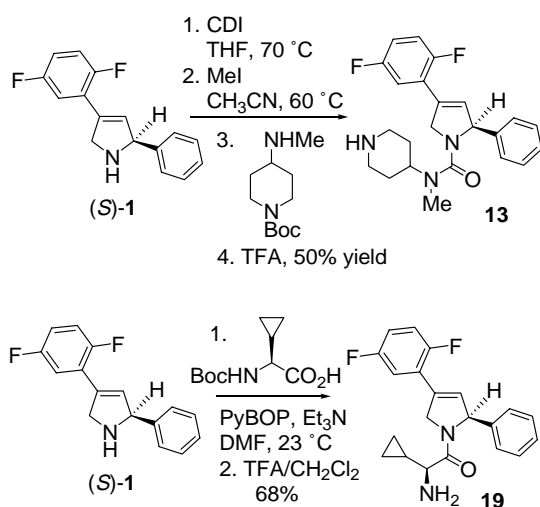
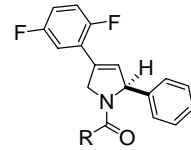
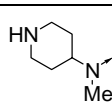
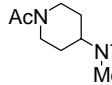
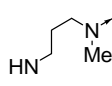
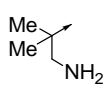
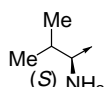
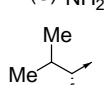
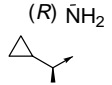
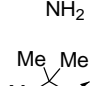
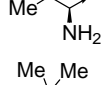
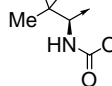


Figure 4. Synthesis of **13** and **19** from (*S*)-**1**.

Table 2. Properties of dihydropyrroles **13–22**



Compound	R	KSP IC <sub>50</sub> (nM)	Cell EC <sub>50</sub> (nM)	HERG IC <sub>50</sub> (nM)
<b>13</b>		2.6	6.8	1300
<b>14</b>		50	69	>10,000
<b>15</b>		16	44	1300
<b>16</b>		5.2	11	2200
<b>17</b>		3.6	12	2400
<b>18</b>		3100	ND	ND
<b>19</b>		2.0	8.6	3500
<b>20</b>		2.7	7.1	1500
<b>21</b>		7.4	13	25,000
<b>22</b>		11	20	11,000

ND, not determined.

Comparative analysis of the X-ray crystal structures of compounds **13** and **19** with **6** provided possible explanations for their differences in KSP inhibitory activity (Fig. 5).<sup>19</sup> In the structure of **13**, the piperidinyll group projects away from the hydrophobic regions of the allosteric pocket to place the basic nitrogen at the polar solvent front, minimizing the energy cost of desolvation. Interestingly, this preference gives rise to a rotamer conformation for the urea moiety that is transposed relative to urea **6**. Adoption of this rotamer conformation directs the methyl group of **13** into a hydrophobic region just below the plane of the dihydropyrrole core, further increasing the binding energy.<sup>20</sup> Similarly with **19**, positioning of the primary amino group at the solvent interface has the effect of directing the lipophilic cyclopropyl sidechain into this hydrophobic region, and thus offers an explanation for the requirement of

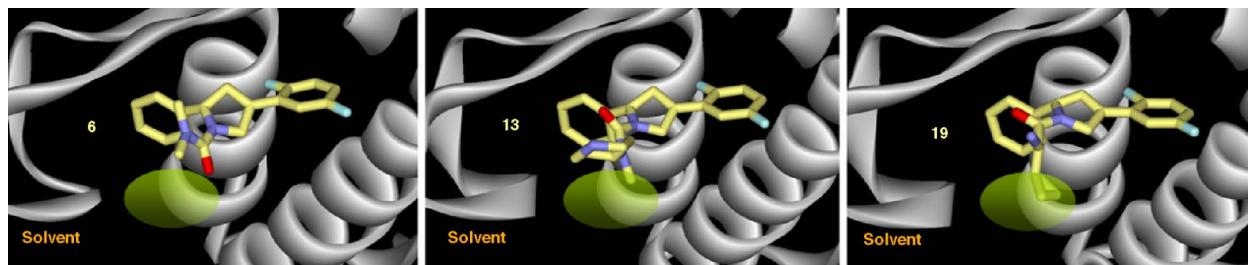
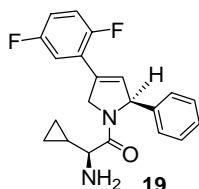


**Figure 5.** Crystal structures of **6**, **13** and **19** bound to the allosteric site of KSP. Protein shown in solid ribbon. Green patch indicates location of a hydrophobic region in the binding site.

**Table 3.** Pharmacokinetic profile of **19** following iv dosing to animals



Species	Dose (mg/kg)	Cl (mL/min/kg)	$V_{dss}$ (L/kg)	$t_{1/2}$ (h)
Rat ( $n = 4$ )	1.0	$40 \pm 5.8$	$4.4 \pm 1.5$	$1.4 \pm 0.4$
Dog (4)	0.4	$23 \pm 4.5$	$3.8 \pm 0.3$	$2.3 \pm 0.3$
Monkey (3)	0.4	$21 \pm 2.5$	$7.4 \pm 0.8$	$4.5 \pm 0.8$

the *S* stereochemical configuration of the  $\alpha$ -amino amides for optimal potency.

The pharmacokinetic profile of compound **19** in rat, dog, and monkey following iv administration is presented in Table 3 and was representative of the series. Plasma clearance was moderate in these species with half-lives ranging from 1 to 4 h, respectively.

In summary, we have described the development of dihydropyrroles as novel and potent KSP inhibitors through core modification of dihydropyrazole-based lead structures. Potency and aqueous solubility were gained simultaneously through the introduction of basic amides and ureas, a key finding from our optimization efforts. In addition, it was discovered that the moderate level of hERG binding demonstrated by the basic inhibitors could be attenuated through the use of charge-neutral acyl groups.

### Acknowledgments

We thank Dr. Harry Ramjit for high resolution mass spectral analysis, Carl Homnick for chiral separation to give **6**, and Dr. Laszlo Kiss for cellular electrophysiological evaluation of **19** on hERG.

### References and notes

- For reviews, see: (a) Heald, R. *Cell* **2000**, *102*, 399; (b) Sharp, D. J.; Rogers, G. C.; Scholey, J. M. *Nature* **2000**, *407*, 41; (c) Endow, S. A. *Eur. J. Biochem.* **1999**, *262*, 12.
- Blangy, A.; Lane, H. A.; d'Hérin, P.; Harper, M.; Kress, M.; Nigg, E. A. *Cell* **1995**, *83*, 1159.
- Mayer, T. U.; Kapoor, T. M.; Haggarty, S. J.; King, R. W.; Schreiber, S. L.; Mitchison, T. J. *Science* **1999**, *286*, 971.
- Marcus, A. I.; Peters, U.; Thomas, S. L.; Garrett, S.; Zelnak, A.; Kapoor, T. M.; Giannakakou, P. *J. Biol. Chem.* **2005**, *280*, 11569.
- Tao, W.; South, V. J.; Zhang, Y.; Davide, J. P.; Farrell, L.; Kohl, N. E.; Sepp-Lorenzino, L.; Lobell, R. B. *Cancer Cell* **2005**, *8*, 49.
- For reviews, see: (a) Duhl, D. M.; Renhowe, P. A. *Curr. Opin. Drug Discov. Dev.* **2005**, *8*, 431; (b) Coleman, P. J.; Fraley, M. E. *Expert Opin. Ther. Patents* **2004**, *14*, 1659.
- Cox, C. D.; Breslin, M. J.; Mariano, B. J.; Coleman, P. J.; Buser, C. A.; Walsh, E. S.; Hamilton, K.; Huber, H. E.; Kohl, N. E.; Torrent, M.; Yan, Y.; Kuo, L. C.; Hartman, G. D. *Bioorg. Med. Chem. Lett.* **2005**, *15*, 2041.
- Carpes, M. J. S.; Correia, C. R. D. *Synlett* **2000**, *9*, 1037.
- All compounds were characterized by  $^1\text{H}$  NMR and high resolution mass spectrometry. For detailed experimental procedures, see WO03105855.
- KSP inhibitory activity was assessed by measuring the release of inorganic phosphate from ATP hydrolysis through absorbance detection of a quinaldine red-phosphate complex. For assay details, see: Cogan, E. B.; Birell, G. B.; Griffith, O. H. *Anal. Biochem.* **1999**, *271*, 29,  $\text{IC}_{50}$  values are reported as the averages of at least two independent determinations; standard deviations are within  $\pm 25$ –50% of  $\text{IC}_{50}$  values.
- The KSP  $\text{IC}_{50}$  for the (+, *R*) enantiomer of **6** was determined to be  $>50,000$  nM.
- Compound **8** was prepared from (*S*)-epichlorohydrin by modification of the method of Sassaman, M. B.; Prakash, G. K. S.; Olah, G. A. *J. Org. Chem.* **1990**, *55*, 2016.
- Maeda, K.; Yamamoto, Y.; Tomimoto, K.; Mase, T. *Synlett* **2001**, 1808.
- Interestingly, use of LiHMDS under the same reaction conditions produced a 2:1 mixture of enol triflates, favoring **11**.
- As with the dihydropyrazoles, the 2,5-difluorophenyl ring was found to be optimal in the dihydropyrrole series (data not shown).
- Mitotic arrest was measured by assessing the mitosis-specific phosphorylation of nucleolin using an antibody-coated, bead-based assay. In this assay, total nucleolin is captured on a streptavidin-coated paramagnetic bead coupled with biotinylated nucleolin monoclonal IgG1 antibody 4E2 (Research Diagnostics, Inc.). Nucleolin phosphorylation is detected by an antibody complex consisting of a phospho-specific nucleolin IgM monoclonal antibody, TG3 (Applied NeuroSolutions, Inc.) and a goat anti-mouse IgM labeled with a ruthenium Tris-bipyridyl complex (BV-TAG Technology, BioVeris Corp.). The complex is quantitated via

electrochemiluminescence based on the excitation/emission properties of the Tris-bipyridyl complex using a BioVeris M-series analyzer. EC<sub>50</sub> for KSP-induced nucleolin phosphorylation was determined after treatment with a compound in a 7-point, half-log dilution series for 16 h. The values of EC<sub>50</sub> are reported as the average of at least two independent determinations; standard deviations are within ±25–50% of EC<sub>50</sub> values.

17. The hERG IC<sub>50</sub> values are reported as the average of at least two independent determinations and were acquired

by radioligand binding competition experiments using membrane preparations from human embryonic kidney cells that stably express hERG. For assay details, see: Bilodeau, M. T. et al. *J. Med. Chem.* **2004**, *47*, 6363, and references therein.

18. Roden, D. M. *N. Engl. J. Med.* **2004**, *350*, 1013.

19. PDB deposition numbers for **6**, **13**, and **19**: 2FL6, 2FKY, and 2FL2, respectively.

20. Hydrophobic grids were calculated on an SGI and generated using a Morse potential and a Lennard-Jones repulsive VdW.